# A General Markov Random Field Model by Partial Differential Equations Method

Huawu Deng, Jun Liu
School of Electrical and Electronic Engineering
Nanyang Technological University
Singapore 639798
P144931257@ntu.edu.sg, ejliu@ntu.edu.sg

**Abstract**

Markov Random Field(MRF) is efficient to model texture images, and many applicable models have been developed. The interpretations of these available models provide many different views of the image model structure and their application. In this paper, we present a new MRF model called PDE-MRF model based on constructing generic energy function by Partial Differential Equations(PDE) method. This model not only includes the majority of the present particular MRF models but also is a uniform template to develop some new models.

KEYWORDS: Markov Random Field (MRF), Texture Modeling, Partial Differential Equations (PDEs), PDE-MRF Model, Energy Function

## 1 Introduction

**Markov Random Field(MRF)** was introduced into image processing by J. Besag[1], and it has been applied to a lot of practical problems. Such fields of image processing as image restoration, image segmentation and image classification employ MRF model as one of their main tools. Among these applications, texture analysis, texture modeling are two important and fruitful fields.

Generally, texture generation process involves a stochastic assumption[2]. The gray level at a point in a texture image is highly dependent on the gray levels of neighboring points unless the image is simply random noise. MRF is able to describe this dependence. According to variable kinds of textures and applications, many particular MRF models have been presented, e.g., Auto Models(including Auto-Logistic model, Auto-Binomial model, Auto-Normal model and Auto-Poisson model)[1], Multi-Level Logistic Model(MLL)[3], Hierarchical GRF Model[4], and FRAME[5]. These models have different structures, and their parameters are determined not mainly by the texture types but by experiments of goodness-of-fit of the observed texture and the generated one. As a result, randomness is inconsistently added to the structure of the model and definition of the parameters.

**Partial Differential Equation(PDE)** methods have been applied to image representation for nearly forty years. A. Turing is the researcher who first used PDE model to synthesize animal patterns, in which the method is called as reaction-diffusion[6]. A general outline of relations between PDE and image processing was presented by A. K. Jain in his paper[7]. After introducing the notion scale-space into PDE methods by Koenderink[8] and Witkin[9], several PDE models for image processing have been created, for example, anisotropy-diffusion PDE models by Perona and Malik[10], anisotropy reaction-diffusion by Witkin and Kass[11] and so on. These models not only focus on image restoration or edge detection but also can be applied to texture analysis.

The reasons for many applications of PDE models to image processing are rooted in the advantages of PDEs. First, PDEs can satisfy such stability requirements for image processing as locality and causality. Second, the PDE formulation is natural in order to combine algorithms. Another important advantage of the PDE approach is the possibility of achieving high accuracy and stability aided by available numerical analysis.

It is noted that PDEs mainly possess deterministic property that is always corrupted by uncertainties in image data. Another problem is the inflexibility of choosing coefficients and equation forms. A realistic image model should integrate the known deterministic

characteristics which can be represented by PDE models and the uncertainties which can be represented by MRF models[12].

## 2 Structure of PDE-MRF Model

A generic contextual constraint on the real world is smoothness. It assumes that physical properties in a neighborhood of space or in an interval of time present some coherence and generally do not change abruptly. Smoothness constrains are often expressed as the prior probability of equivalently an energy measuring the extent to which the smoothness assumption is violated[13].

In GRF/MRF, the energy is the function of image data. In order to capture the features in image, the specific energy function should approximate the real energy of image to the maximized extent. Based on the consideration of smoothness-prior assumption for texture images and the deterministic properties of PDEs, a suitable form of energy function can be constructed with part of PDEs such as partial differential operators within potential functions.

The general energy function of a neighborhood region can be of such form as:

$$V_C = \int\int_N [f_1(\frac{\partial I}{\partial x}) + f_2(\frac{\partial I}{\partial y}) + f_3(\frac{\partial^2 I}{\partial x^2}) + f_4(\frac{\partial^2 I}{\partial y^2}) + f_5(I)]dxdy \quad (1)$$

where $f_1, f_2, f_3, f_4$ and $f_5$ are continuous functions, $N$ is the neighborhood region, $\frac{\partial I}{\partial x}$, $\frac{\partial I}{\partial y}$, $\frac{\partial^2 I}{\partial x^2}$ and $\frac{\partial^2 I}{\partial y^2}$ are the partial derivatives, and $I$ is the image.

The selected functions for the operators are to enhance or suppress such texture properties as edges, smoothness, roughness and so on. The part $\{f_1(\frac{\partial I}{\partial x}) + f_2(\frac{\partial I}{\partial y}) + f_3(\frac{\partial^2 I}{\partial x^2}) + f_4(\frac{\partial^2 I}{\partial y^2}) + f_5(I)\}$ is actually a part of PDEs and its variation complies with PDEs. So this kind of energy functions are deterministic.

The discrete form of the general energy function can be deduced, for example, by operating the partial operators on the cliques of the second order neighborhood. As a result, the discrete forms of these partial differential operators are the first order and second order finite difference, which reflect the difference of gray level between neighboring sites.

Here we use both forward and backward finite difference to discretize the partial differential operators in order to comply with the neighborhood system. In the second-order neighborhood, $\frac{\partial I}{\partial x}$ is denoted by $(I_{i,j+1} - I_{i,j})$ or $(I_{i,j-1} - I_{i,j})$ with respect to the horizontal pair-site cliques; $\frac{\partial I}{\partial y}$ is denoted by $(I_{i+1,j} - I_{i,j})$ or $(I_{i-1,j} - I_{i,j})$ with respect to the vertical pair-site cliques. For the diagonal pair-site cliques, $\frac{\partial I}{\partial x}$ and $\frac{\partial I}{\partial y}$ can be denoted by $\frac{\sqrt{2}}{2}(I_{i+1,j+1} - I_{i,j})$ or $\frac{\sqrt{2}}{2}(I_{i-1,j-1} - I_{i,j})$ or $\frac{\sqrt{2}}{2}(I_{i+1,j-1} - I_{i,j})$ or $\frac{\sqrt{2}}{2}(I_{i-1,j+1} - I_{i,j})$. Therefore, a general form to represent $f_1(\frac{\partial I}{\partial x})$ and $f_2(\frac{\partial I}{\partial y})$ over all pair-site cliques is $f_1(I_{i',j'} - I_{i,j})$ when $f_1$ and $f_2$ are selected as identical function (actually, $f_1$ and $f_2$ are often of same form due to operating on pair-site cliques). Let $(I_{i-1,j} - 2I_{i,j} + I_{i+1,j})$ denote $\frac{\partial^2 I}{\partial y^2}$, and $(I_{i,j-1} - 2I_{i,j} + I_{i,j+1})$ denote $\frac{\partial^2 I}{\partial x^2}$, and then the discrete form of $V_C$ is:

$$\begin{aligned} V_C = & \sum_{(i',j')\in c, c\in C} f_1(I_{i',j'} - I_{i,j}) \\ & + f_3(I_{i,j-1} - 2I_{i,j} + I_{i,j+1}) \\ & + f_4(I_{i-1,j} - 2I_{i,j} + I_{i+1,j}) \\ & + f_5(I_{i,j}). \end{aligned} \quad (2)$$

In (2), the second item and third one may be omitted if functions $f_1, f_3$ and $f_4$ are identical. But if the functions are chosen differently, these two items play an important role in the energy function and can not be ignored. The conditional probability distribution of PDE-MRF model is given by:

$$P\{I_{i,j}|N_{i,j}\} = \frac{e^{-V_C}}{\sum_{I'_{i,j}} e^{-V_C}}, \quad (3)$$

where $I'_{i,j}$ is any possible gray level and $V_C$ is denoted in (2). Equation (3) reflects the Markovianity. Therefore, PDE-MRF model is an integration of PDE models and MRF models.

Equation (2) is a very general energy function form. It can be explained that it reflects the gray level difference between neighboring sites whose variations are shaped by potential function. By selecting some functions for $f_1, f_3, f_4$ and $f_5$, we can obtain certain number of MRF models including traditional MRF models and new MRF models.

# 3 An MRF Model by PDE-MRF Approach

Many traditional MRF models can be represented by PDE-MRF model through selecting particular energy functions. Here we use only MLL model as a typical example for illustration. The reasons are as follows.

First, this model is used most frequently among all MRF models due to its simple structure and efficient applications. Second, because its clique potential depends on the type(size, shape and possible orientation) of the clique and the local configuration, its potential is difficult to be defined in mathematics in spite of the ease of its description in semantics.

For cliques containing more than one site, the MLL clique potentials are defined by

$$V_c = \begin{cases} \beta_c & \text{if the sites of } c \text{ have the same value} \\ -\beta_c & \text{otherwise} \end{cases} \tag{4}$$

In the discrete energy form of PDE-MRF model, let $f_3 = f_4 = f_5 = 0$ and $f_1$ be of such function form $f(\xi) = w(\xi)(2\delta(\xi) - 1)$, we can get:

$$V_C = \sum_{(i',j') \in c, c \in C} w(I_{i',j'} - I_{i,j})(2\delta(I_{i',j'} - I_{i,j}) - 1), \tag{5}$$

where $w(\xi)$ is a weight function with respect to clique type, e.g., here we can let $w(\xi) = \beta_c$, $\delta(\xi)$ is delta function and its value is 1 if $\xi$=0 otherwise 0.

If $\Delta I_c$ denotes $(I_{i',j'} - I_{i,j})$ and $\beta_c$ denotes the weight function $w(\Delta I_c)$, the above equation can be rewritten as a simple form:

$$V_C = \sum_{c \in C} \beta_c (2\delta(\Delta I_c) - 1). \tag{6}$$

So the MLL model can be composed according to the above function of PDE-MRF model. In the next section, the exponential model can be used to approximate MLL model. Meanwhile, other MRF models can be reconstructed from PDE-MRF model either precisely or approximately, which manifests the generality of PDE-MRF model.

# 4 New Models for Textures

All the currently available texture models can not model all texture images, and the capacity of each model is limited. The complexity of natural textures, therefore, forces researchers to explore new models to precisely represent them. Here, we present several models obtained from PDE-MRF model by selecting certain special functions for special applications.

## 4.1 Linear Model

If we let the functions $f_1, f_3, f_4$ and $f_5$ be constant and the constant is the same with respect to common clique type, then a simple model can be formed. This model is linear, hence termed linear model. The energy function is written as:

$$V_C = \sum_{(i',j') \in c, c \in C} \beta_{i',j'}(I_{i',j'} - I_{i,j}) + \gamma I_{i,j}, \tag{7}$$

where $\alpha_{j'}, \beta_{i'}$ and $\gamma$ are the parameters according to clique type.

In the above energy function, two items $\gamma(I_{i,j-1} - 2I_{i,j} + I_{i,j+1})$ and $\lambda(I_{i-1,j} - 2I_{i,j} + I_{i+1,j})$ are omitted because functions $f_3$ and $f_4$ are also constant like $f_1$ and both items are linear combination of the first item. For example, $\gamma(I_{i,j-1} - 2I_{i,j} + I_{i,j+1}) = \gamma(I_{i,j-1} - I_{i,j}) + \gamma(I_{i,j+1} - I_{i,j})$. Therefore, the addition of the two omitted items only changes the parameters of the energy function without any essential effect on the model structure.

Generally, the finite difference only multiplied by constants without any enhancement or suppression can not capture texture features. Due to the simplicity of this model, the textures it can model are limited.

## 4.2 Non-Negative Models

Take the functions $f_1, f_3$ and $f_4$ as the absolute value of the partial derivatives and assign constants as weights to these functions with respect to clique type, and let $f_5 = 0$, we can get the energy function like:

$$\begin{aligned} V_C = & \sum_{(i',j') \in c, c \in C} \beta_{i',j'} |I_{i',j'} - I_{i,j}| \\ & + \gamma |I_{i,j-1} - 2I_{i,j} + I_{i,j+1}| \\ & + \lambda |I_{i-1,j} - 2I_{i,j} + I_{i+1,j}|, \end{aligned} \tag{8}$$

where $\beta_{i',j'}, \gamma$ and $\lambda$ are the parameters with respect to clique types. Comparing with the linear model, we preserve the second and third items because they can not be decomposed into the first item but can measure the contrast among three neighboring sites which is impossible to be captured by the first item.

This model is called as Non-Negative model. If the selected function is quadratic function, we can form another Non-Negative model. The non-negative property of these models can describe roughness and smoothness of texture.

## 4.3 Exponential Model

Let the functions $f_1$ be $f(\xi) = 2e^{-2\xi^2} - 1$ and other functions be zero, we obtain the exponential model. Assigned weights to every function with respect to clique type, the energy function can be given by:

$$V_C = \sum_{(i',j')\in c, c\in C} \beta_{i',j'}(2e^{-2(I_{i',j'}-I_{i,j})^2} - 1). \quad (9)$$

Let $\Delta I_c$ denote $(I_{i,j'} - I_{i,j})$, and $\beta_c$ denote the parameters $\beta_{i',j'}$, the above energy function can be rearranged as follows:

$$V_C = \sum_{c\in C} \beta_c(2e^{-2(\Delta I_c)^2} - 1). \quad (10)$$

This form is similar to equation (6). So this exponential model is much similar to the MLL model except the minor difference that the discrete jump is replaced by a continuous exponential function with nearly same effects.

Assumed that the neighborhood system is the second order and assigned the same weights to the same clique types, the concrete form of (10) is:

$$\begin{aligned} V_C &= \beta_1(e^{-2(I_{i-1,j-1}-I_{i,j})^2} + e^{-2(I_{i+1,j+1}-I_{i,j})^2} - 1) \\ &+ \beta_2(e^{-2(I_{i-1,j+1}-I_{i,j})^2} + e^{-2(I_{i+1,j-1}-I_{i,j})^2} - 1) \\ &+ \beta_3(e^{-2(I_{i,j-1}-I_{i,j})^2} + e^{-2(I_{i,j+1}-I_{i,j})^2} - 1) \\ &+ \beta_4(e^{-2(I_{i-1,j}-I_{i,j})^2} + e^{-2(I_{i+1,j}-I_{i,j})^2} - 1). \quad (11) \end{aligned}$$

This energy function will be used in the followed experiments.

## 4.4 Potential Model

Also we can use a potential function like $f(\xi) = 1 - \frac{1}{1+(\|\xi\|/b)^r}$ as the form of $f_1, f_3, f_4$ and $f_5$. This kind of functions $f(\xi)$ owns a good property of enhancing the edge information in texture image. The energy function is formed as:

$$\begin{aligned} V_C &= \sum_{(i',j')\in c, c\in C} \beta_{i',j'}(1 - \frac{1}{1+(\| I_{i,j'} - I_{i,j} \| /b)^r}) \\ &+\gamma(1 - \frac{1}{1+(\| I_{i,j-1} - 2I_{i,j} + I_{i,j+1} \| /b)^r}) \\ &+\lambda(1 - \frac{1}{1+(\| I_{i-1,j} - 2I_{i,j} + I_{i+1,j} \| /b)^r}) \\ &+\zeta(1 - \frac{1}{1+(\| I_{i,j} \| /b)^r}), \quad (12) \end{aligned}$$

where $\beta_{i',j'}, \gamma, \lambda$ and $\zeta$ are the parameters according to clique types.

Models constructed in such way belong to potential models. By analyzing the characteristics of nature texture images by statistical methods or other tools, more suitable potential functions can be achieved and be employed in the potential models.

## 4.5 Hybrid Potential Model

In each of the above models, we use only one potential function for all partial differential operators. This way to construct the energy function certainly limits the capacity of the formed model for modeling textures. Actually, each operator in the energy function of PDE-MRF model plays different roles, so the major function of each operator should be enhanced by certain potential function. By this consideration, we want to construct the energy function using two different potential functions. Models formed in such way are termed Hybrid Potential Model.

Let $f_1$ be $f(\xi) = 2e^{-2\xi^2} - 1$, and $f_3, f_4$ and $f_5$ be $f'(\xi) = \log(\cosh(\xi))$(cosh is hyperbolic cosine function), the discrete energy function is formed as:

$$\begin{aligned} V_C &= \sum_{(i',j'\in c, c\in C} \beta_{i',j'}(2e^{-2(I_{i',j'}-I_{i,j})^2} - 1) \\ &+\gamma\log(\cosh(I_{i,j-1} - 2I_{i,j} + I_{i,j+1})) \\ &+\lambda\log(\cosh(I_{i-1,j} - 2I_{i,j} + I_{i+1,j})) \\ &+\zeta\log(\cosh(I_{i,j})). \quad (13) \end{aligned}$$

In mathematics, $f(\xi) = 2e^{-2\xi^2} - 1$ is nonconvex function that tends to result in sharp discontinuities, while $f'(\xi) = \log(\cosh(\xi))$ is convex function which often allows global optimization. So this model is hybrid in two aspects: different potential function forms and different properties of each function.

## 5 Experiments and Results

Based on the discrete energy function form of linear model, we can synthesize texture images by sampling from (3). The texture shown in image (a) of figure 1 is dominated by lower gray values and the brighter pixels do not cluster due to more weights on single sites. Image (b) of figure 1, also sampled from the linear model with different parameters from image (a), is almost noise, which shows the limited capacity of linear model.

The second experiment is made in the case of exponential model. From the results shown in the figure 2, its performance is the same as the MLL model. But minor difference exists between the corresponding images modeled by exponential model and MLL model respectively, since the selected function is continuous and thus takes advantages over the discrete function used by MLL model. This results in stronger capacity of the exponential model than that of MLL model.

The third experiment is conducted on the condition of using $f(\xi) = 1 - \frac{1}{1+(\|\xi\|/b)^r}$ as the energy function form. The image in the first row of figure 5 is generated with $b = 2$ and $r = 1.2$. Based on more experimental results that are not shown in this report, we find many of textures modeled by this model are similar to those modeled by the exponential model. The reason is that both functions $f(\xi) = 2e^{-2\xi^2} - 1$ and $f'(\xi) = 1 - \frac{1}{1+(\|\xi\|/b)^r}$ are nonconvex. From the curves in figure 3 and 4, the former function approximates a linear transformation of the latter function, e.g., $f(\xi) \approx 1 - f'(\xi)$ when $b = 2, r = 1.2$. This linear transform can be aligned by setting corresponding parameter values in the energy function. Of course, some new textures can be synthesized when $r$ and $b$ are set to other special values such as $b = 5, r = 5$ and so forth.

The forth experiment is done by using the hybrid potential model. Besides generating the textures modeled by the exponential model, it can model new texture shown in the first row of figure 5. The new features captured by it is caused by combination of a nonconvex function and a convex function. It is not a fiction that the capacity of this model can be strengthened and greatly extended by using more that two potential functions in the energy function.

Due to integrating both deterministic characteristics such as edges and smoothness of PDE methods and uncertainty of MRF models, the PDE-MRF model is a generalization of MRF model.

## 6 Discussions and Conclusion

In the PDE-MRF model, the energy function is considered as the variation of energy distribution according to the PDEs, which denote the way to achieve equilibrium. If the energy converges, the conditional probability of MRF model reaches the maximum and texture pattern forms. Because the construction of energy function in the PDE-MRF model is based on the assumption of smoothness constrain, though permitted some violations for texture patterns, and other constrains for texture such as regularization are ignored or suppressed, PDE-MRF model can only model limited number of texture types. Another problem for PDE-MRF model is how to relate the selected functions to image features, for the form of functions has great effects on pattern formation. To learn from the histogram of nature images is one applicable way, but other methods must be explored in the future. The future challenge of improving PDE-MRF model includes two aspects. One is to find which constrains are suitable for describing textures and how to apply them to the energy function; another is how to learn the function forms in PDE-MRF model.

In a conclusion, the capacity of MRF models and PDE models is limited to describe textures if they are used independently, but the integration of the advantages of both models can enhance their capacity greatly.

## References


[1] J. E. Besag, "Spatial Interaction and the Statistical Analysis of Lattice Systems (with Discussion)," *Royal Stat. Soc.*, vol. B-36, pp. 192–236, 1974.

[2] G. R. Cross and A. K. Jain, "Markov Random Field Texture Models," *IEEE Trans. Pattern Anal. Machine Intell.*, vol. 5, no. 1, pp. 44–58, 1983.

[3] H. Elliott, H. Derin, R. Cristi, and D. Geman, "Application of the Gibbs Distribution to Image Segmentation," *Proc. Intl. Conf. Acoustic, Speech and Signal Processing, San Diego*, vol. 32, pp. 1–4, 1984.

[4] H. Derin and W. S. Cole, "Segmentation of Textured Images Using Gibbs Random Fields," *Computer Vision, Graphics and Image Processing*, vol. 35, pp. 72–98, 1986.

[5] S. C. Zhu and D. Mumford, "Filters, Random Fields and Maximum Entropy(FRAME)–Towards A Unified Theory for Texture Modeling," *Int'l Journal of Computer Vision*, vol. 27, no. 2, pp. 1–20, 1996.

[6] A. Turing, "The Chemical Basis of Morphogenesis," *Philosophical Transactions of the Royal Society B*, vol. 237, pp. 37–72, 1952.

[7] A. K. Jain, "Partial Differential Equations and Finite-Difference Methods in Image Processing. Part I: Image Representation," *Journal Optimization Theory And Applications*, vol. 23, no. 9, pp. 65–91, 1977.

[8] J. J. Koenderink, "The Structure of Images," *Biol. Cybern*, vol. 50, pp. 363–370, 1984.

[9] A. P. Witkin, "Scale-Space Filtering," *Proc. Int. Joint Conf. Artif. Intell.*, vol. 1, pp. 1019–1021, 1983.

[10] P. Perona and J. Malik, "Scale-Space and Edge Detection Using Anisotropic Diffusion," *IEEE Trans. Pattern Anal. Machine Intell.*, vol. 12, no. 7, pp. 629–639, 1990.

[11] A. Witkin and M. Kass, "Reaction-Diffusion Textures," *Computer Graphics*, vol. 25, no. 4, pp. 299–308, 1991.

[12] R. Chellappa and A. A. Sawchuk, *Digital Image Processing and Analysis*, vol. I, IEEE Computer Society, Los Angeles, USA, 1985.

[13] S. Z. Li, *Markov Random Field Modeling in Computer Vision*, New York: Springer-Verlag, 1995.

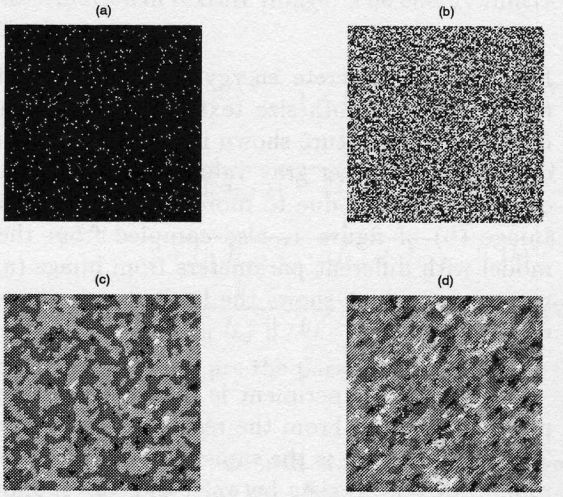


Figure 1: Synthesized images by PDE-MRF model: (a) function form is constant, and the parameters $\alpha_1 = -1, \alpha_2 = -1, \beta_1 = -2, \beta_2 = -2, \gamma = 0$; (b)function form is constant, and the parameters $\alpha_1 = 1, \alpha_2 = -1, \beta_1 = -1, \beta_2 = 2, \gamma = 2$; (c)function form is absolute value, an the parameters $\alpha_1 = 1, \alpha_2 = 1, \beta_1 = 1, \beta_2 = 2, \gamma = 1, \lambda = 1$; (d) function form is absolute value, and the parameters $\alpha_1 = 1, \alpha_2 = 1, \beta_1 = 1, \beta_2 = 2, \gamma = -1, \lambda = -1$

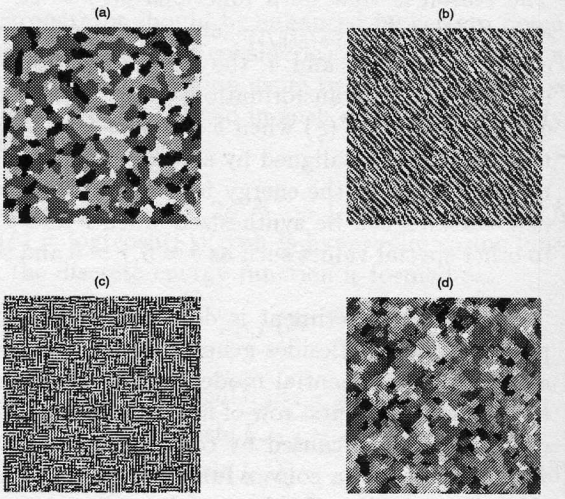


Figure 2: Synthesized images by exponential model: (a) $M$(gray level)= 3, $\alpha_1 = 1, \alpha_2 = 1, \beta_1 = 1, \beta_2 = 1$, (b) $M = 4$, $\alpha_1 = 1, \alpha_2 = 1, \beta_1 = 1, \beta_2 = -1$, (c) $M = 4$, $\alpha_1 = -1, \alpha_2 = -1, \beta_1 = -1, \beta_2 = -1$, (d) $M = 4$, $\alpha_1 = -1, \alpha_2 = -1, \beta_1 = 2, \beta_2 = 2$

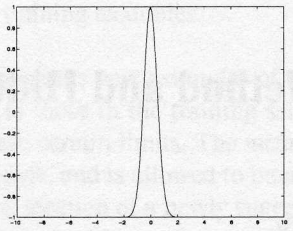

Figure 3: Curve of $f(\xi) = 2e^{-2\xi^2} - 1$

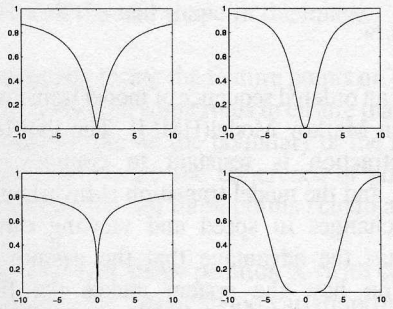

Figure 4: Curves of $f(\xi) = (1 - \frac{1}{1+(\|\xi\|/b)^r})$ with different values of parameters: Upper-left with b=2, r=1.2; Upper-right with b=2, r=2; Lower-left with b=0.5, r=0.5; Lower-right with b=5, r=5

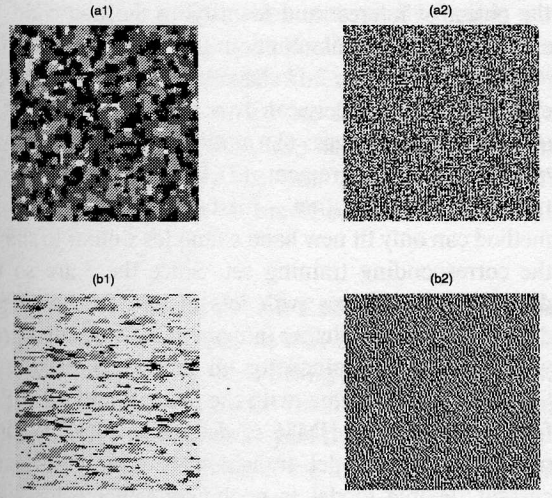


Figure 5: Synthesized images by Potential model and Hybrid Potential model: (a1) by Potential model with $\beta_1 = -1.4, \beta_2 = -1.4, \beta_3 = 0.3, \beta_4 = 0.2, \gamma = 1.4, \lambda = 1.5, \zeta = 0.8$; (b1) by Potential model with $\beta_1 = 0.3, \beta_2 = 0.4, \beta_3 = 0.5, \beta_4 = 0.6, \gamma = 1.2, \lambda = 0.2, \zeta = 2$; (b2) by Hybrid Potential model with $\beta_1 = -2, \beta_2 = -0.1, \beta_3 = -0.1, \beta_4 = -0.1, \gamma = 0, \lambda = 0, \zeta = -1$;(b1) by Hybrid Potential model with $\beta_1 = 2, \beta_2 = -0.1, \beta_3 = -0.2, \beta_4 = 2, \gamma = -2, \lambda = -2, \zeta = 0$